Effect of bending-twisting coupling on the compression and shear buckling strength of infinitely long plates

Christopher Bronn York[1*] and Sergio Frascino Muller de Almeida [2]

[1] Aerospace Sciences, School of Engineering, University of Glasgow, University Avenue, G12 8QQ, Glasgow, Scotland.

[2] Department of Mechatronics and Mechanical Systems Engineering, University of São Paulo, Av. Professor Mello Moraes, 2231, São Paulo, SP, 05508-030, Brazil.

Abstract

This article describes the development of closed form polynomial equations for compression and shear buckling to assess the effect of *Bending-Twisting* coupling on infinitely long laminated plates with simply supported edges. The equations are used to generate contour maps, representing non-dimensional buckling factors, which are superimposed on the lamination parameter design spaces for laminates with standard ply orientations. The contour maps are applicable to two recently developed databases containing symmetric and non-symmetric laminates with either *Bending-Twisting* or *Extension-Shearing Bending-Twisting* coupling. The contour maps provide new insights into buckling performance improvements that are non-intuitive and facilitate comparison between hypothetical and practical designs. The databases are illustrated

[*]Corresponding author: Tel: +44 (0)141 3304345, E-mail address: Christopher.York@Glasgow.ac.uk

through point clouds of lamination parameter coordinates, which demonstrate the effect of applying common design heuristics, including ply angle, ply percentage and ply contiguity constraints.

Keywords

Extension-Shearing, Bending-Twisting coupling; Buckling contours; Closed form solutions; Compression Buckling; Lamination Parameters; Laminate Stacking Sequences; Shear Buckling.

Nomenclature

$\mathbf{A}$, A_{ij} = extensional stiffness matrix and its elements, $i,j = x, y, s$

$\mathbf{D}$, D_{ij} = bending stiffness matrix and its elements, $i,j = x, y, s$

$E_{1,2}$, G_{12} = in-plane Young's moduli and shear modulus

H = laminate thickness (= number of plies, $n \times$ ply thickness, t)

N_x, N_s = compression and shear buckling load (N/mm)

k_x, k_s = non-dimensional buckling load factor for compression and shear

n = number of plies in laminate stacking sequence

Q_{ij} = reduced stiffness elements

t = ply thickness

U_E, U_G = laminate invariants for equivalent isotropic properties, E_{Iso} and G_{Iso}

U_Δ, U_R = laminate invariants for orthotropic properties

x,y,z = principal axes

λ = buckling half-wave

ν_{ij} = Poisson ratio

$\xi_{\Delta}^{A}, \xi_{R}^{A}$ = lamination parameters for orthotropic extensional stiffness

$\xi_{\Delta c}^{A}, \xi_{Rc}^{A}$ = lamination parameters for coupled extensional stiffness

$\xi_{\Delta}^{D}, \xi_{R}^{D}$ = lamination parameters for orthotropic bending stiffness

$\xi_{\Delta c}^{D}, \xi_{Rc}^{D}$ = lamination parameters for coupled bending stiffness

1. Introduction

The effect of *Bending-Twisting* coupling continues to be ignored in studies relating to the buckling performance of plate or panel structures, which is broadly justified on the basis that the effects dissipate for laminates with a large number of plies. However, there is a significant body of research demonstrating that compression buckling strength may be overestimated (unsafe) and shear buckling strength may be overestimated or underestimated (over-designed) if the effects of *Bending-Twisting* coupling are ignored.

In this study, the effect of *Bending-Twisting* coupling on infinitely long laminated plates with simply supported edges is investigated, which complements an extensive literature on the subject, where the focus is primarily on finite length plates.

The relative buckling performance of adopting non-symmetric laminate designs is also revealed. With very few exceptions, the study of *Bending-Twisting* coupling effects has focussed entirely on symmetric designs.

Recent research has led to laminate design databases containing *Extension-Shearing* [1] and/or *Bending-Twisting* coupling [2]. The results have demonstrated that the design spaces contain predominantly non-symmetric stacking sequences. All are immune to

thermal warping distortions by virtue of the fact that their coupling stiffness properties are null (**B** = **0**), as would be expected from symmetric laminate configurations. Heuristic design rules [3] are now applied to these databases to assess the effect on optimum buckling performance of practical rather than hypothetical designs. The reduction in the design space is readily quantified through graphical representation of the lamination parameter design space.

New insights into compression and shear buckling strength are provided via buckling factor contour maps, which are superimposed onto the lamination parameter design spaces. Contour mapping is applied to cross-sections through the design space, to allow detailed interrogation of the effects of *Bending-Twisting* coupling on buckling strength. The mapping is also applied to external surfaces of the feasible domain of lamination parameters, since these surfaces represent the bounds on buckling strength. The results are applicable to infinitely long plates with simply supported edges, which represent useful lower-bound solutions for preliminary design optimisation.

Notable contributions addressing infinitely long plates [4,5] adopted non-dimensional parameters, which differ from the lamination parameters used here. More importantly however, the buckling factor results presented were normalised by a bending stiffness parameter, which varies across the designs space, hence buckling performance is not directly comparable. Early studies on finite length plates have also adopted these non-dimensional parameters [6], as have the most recent studies [7], but a separate body of work has adopted lamination parameters [8-10] to aid optimum design. Comparisons with the infinitely long plate results of this study are therefore possible only for aspect ratios that correspond to the asymptotic result.

2. Design space interrogation

Ply angle dependent lamination parameters allow the stiffness terms to be expressed as linear variables within convenient bounds. However, the optimized lamination parameters must be matched to a corresponding laminate configuration within the feasible region, which is aided here by graphical representation of the lamination parameter design spaces [1,2]. In practical design however, heuristic rules are commonly applied, which generally involve constraints on ply percentages, ply contiguity and ply orientations [3].

Elements of the extensional stiffness matrix [**A**] are related to the lamination parameters by:

$$\begin{aligned}\left[\mathbf{A}\right] &= H\begin{bmatrix} U_E+\xi_\Delta^A U_\Delta+\xi_R^A U_R & U_E-2U_G-\xi_R^A U_R & \xi_{\Delta c}^A U_\Delta/2+\xi_{Rc}^A U_R \\ U_E-2U_G-\xi_R^A U_R & U_E-\xi_\Delta^A U_\Delta+\xi_R^A U_R & \xi_{\Delta c}^A U_\Delta/2-\xi_{Rc}^A U_R \\ \xi_{\Delta c}^A U_\Delta/2+\xi_{Rc}^A U_R & \xi_{\Delta c}^A U_\Delta/2-\xi_{Rc}^A U_R & U_G-\xi_R^A U_R \end{bmatrix} \\ &= \begin{bmatrix} A_{xx} & A_{xy} & A_{xs} \\ A_{xy} & A_{yy} & A_{ys} \\ A_{xy} & A_{ys} & A_{ss} \end{bmatrix}\end{aligned} \tag{1}$$

where laminate invariants are defined in terms of the reduced stiffnesses:

$$\begin{aligned} U_E &= \left(3Q_{11}+3Q_{22}+2Q_{12}+4Q_{66}\right)/8 \\ U_G &= \left(Q_{11}+Q_{22}-2Q_{12}+4Q_{66}\right)/8 \\ U_\Delta &= \left(Q_{11}-Q_{22}\right)/2 \\ U_R &= \left(Q_{11}+Q_{22}-2Q_{12}-4Q_{66}\right)/8 \end{aligned} \tag{2}$$

U_E and U_G are invariants associated with the equivalent isotropic properties of the laminate:

$$U_E = E_{iso} \Big/ \left(1 - \nu_{iso}^2\right)$$
$$U_G = G_{iso} \tag{3}$$

where E_{iso}, G_{iso} and ν_{iso} are the equivalent isotropic properties of the composite material, defined as:

$$E_{iso} = 2(1 + \nu_{iso})G_{iso}$$

$$G_{iso} = (Q_{11} + Q_{22} - 2Q_{12} + 4Q_{66})/8 \tag{4}$$

$$\nu_{iso} = (Q_{11} + Q_{22} + 6Q_{12} - 4Q_{66})/(3Q_{11} + 3Q_{22} + 2Q_{12} + 4Q_{66}) = 1 - 2U_G/U_E$$

U_Δ is associated with orthotropy along axes 1 and 2, i.e. parallel and perpendicular to the fibre direction.

U_R has a complex physical meaning. It is a residual property contained in all elements of the stiffness matrix and is a function of A_{xx}, A_{xy} and A_{ss}. It also produces square symmetry, i.e., $A_{xx} = A_{yy}$, when the lamination parameter $\xi_\Delta^A = 0$. In this case, U_Δ is rendered zero, $A_{ss} = (A_{xx} - A_{xy})/2$ corresponds to $-\xi_R^A$ and, for off axis orientation of a laminate, β, containing standard ply angles $(0 + \beta)$, $(90 + \beta)$, $(45 + \beta)$ and $(-45 + \beta)$, $A_{xs} = -A_{ys}$. When $\xi_\Delta^A = \xi_R^A = 0$, $A_{ss} = G_{iso}H$.

The above equations are identical to the original equations [11]. Only the notation has been reformulated. The authors believe that this new notation is more intuitive, as it refers to the physical interpretation of the invariants and lamination parameters. Also, since there are only two material properties for an isotropic material, only two invariants (U_E and U_G) are used to describe the equivalent isotropic properties of the laminate; the original definition of the lamination parameters uses three invariants (U_1, U_4 and U_5) that are linearly dependent.

The ply orientation dependent lamination parameters are also related to the number of plies, *n*, by the following expressions:

$$\begin{aligned}
\xi_{\Delta}^{A} &= \left[n_{\pm}\left(n_{+}/n_{\pm}\right)\cos\left(2\theta_{+}\right) + n_{\pm}\left(1-n_{+}/n_{\pm}\right)\cos\left(2\theta_{-}\right) \right. \\
&\quad \left. + n_{\mathbf{o}}\cos\left(2\theta_{\mathbf{o}}\right) + \left(n-n_{\pm}-n_{\mathbf{o}}\right)\cos\left(2\theta_{\bullet}\right) \right] / n \\
\xi_{R}^{A} &= \left[n_{\pm}\left(n_{+}/n_{\pm}\right)\cos\left(4\theta_{+}\right) + n_{\pm}\left(1-n_{+}/n_{\pm}\right)\cos\left(4\theta_{-}\right) \right. \\
&\quad \left. + n_{\mathbf{o}}\cos\left(4\theta_{\mathbf{o}}\right) + \left(n-n_{\pm}-n_{\mathbf{o}}\right)\cos\left(4\theta_{\bullet}\right) \right] / n \\
\xi_{\Delta c}^{A} &= \left[n_{\pm}\left(n_{+}/n_{\pm}\right)\sin\left(2\theta_{+}\right) + n_{\pm}\left(1-n_{+}/n_{\pm}\right)\sin\left(2\theta_{-}\right) \right. \\
&\quad \left. + n_{\mathbf{o}}\sin\left(2\theta_{\mathbf{o}}\right) + \left(n-n_{\pm}-n_{\mathbf{o}}\right)\sin\left(2\theta_{\bullet}\right) \right] / n \\
\xi_{Rc}^{A} &= \left[n_{\pm}\left(n_{+}/n_{\pm}\right)\sin\left(4\theta_{+}\right) + n_{\pm}\left(1-n_{+}/n_{\pm}\right)\sin\left(4\theta_{-}\right) \right. \\
&\quad \left. + n_{\mathbf{o}}\sin\left(4\theta_{\mathbf{o}}\right) + \left(n-n_{\pm}-n_{\mathbf{o}}\right)\sin\left(4\theta_{\bullet}\right) \right] / n
\end{aligned} \tag{5}$$

where the subscripts ±, ○ and ● represent ±45°, 0° and 90°, respectively. Note that ξ_{Rc}^{A} = 0 for the standard angle ply configurations chosen here, hence the [**A**] matrix is described by a three dimensional lamination parameter coordinate, which reduces to a two dimensional coordinate if [**A**] is uncoupled.

Elements of the bending stiffness matrix [**D**] have the same form as for the extensional stiffness and are related to the lamination parameters by:

$$\begin{aligned}
\left[\mathbf{D}\right] &= \frac{H^{3}}{12}\begin{bmatrix} U_{E}+\xi_{\Delta}^{D}U_{\Delta}+\xi_{R}^{D}U_{R} & U_{E}-2U_{G}-\xi_{R}^{D}U_{R} & \xi_{\Delta c}^{D}U_{\Delta}/2+\xi_{Rc}^{D}U_{R} \\ U_{E}-2U_{G}-\xi_{R}^{D}U_{R} & U_{E}-\xi_{\Delta}^{D}U_{\Delta}+\xi_{R}^{D}U_{R} & \xi_{\Delta c}^{D}U_{\Delta}/2-\xi_{Rc}^{D}U_{R} \\ \xi_{\Delta c}^{D}U_{\Delta}/2+\xi_{Rc}^{D}U_{R} & \xi_{\Delta c}^{D}U_{\Delta}/2-\xi_{Rc}^{D}U_{R} & U_{G}-\xi_{R}^{D}U_{R} \end{bmatrix} \\
&= \begin{bmatrix} D_{xx} & D_{xy} & D_{xs} \\ D_{xy} & D_{yy} & D_{ys} \\ D_{xs} & D_{ys} & D_{ss} \end{bmatrix}
\end{aligned} \tag{6}$$

Note also that ξ_{Rc}^{D} = 0 for standard ply orientations, hence the [**D**] matrix is described by a three dimensional lamination parameter coordinate for all designs considered here.

2.1 Effect of design heuristics on the lamination parameter design space

Ply percentages are applicable to the design of in-plane properties, which directly affect the extensional stiffness matrix [**A**]. The effect on the bending stiffness design space has not previously been assessed.

Practical design is often based on ply percentages [3], which are readily converted from the associated ply numbers for each orienation. The 10% rule is applied here, which corresponds to the minimum ply percentage for each ply orientation. These percentages can be mapped onto the lamination parameter design space as illustrated on Fig. 1. Figure 1(a) relates ply percentages[†] to the orthotropic parameters, ξ_{Δ}^{A} and ξ_{R}^{A}, and Fig. 1(b) introduces the anisotropic or coupling parameter, ξ_{Rc}^{A}, which is zero in balanced laminates. The commonly applied 10% rule restricts the design space to the central triangular region indicated with broken lines.

Reduced data sets, after applying the 10% rule to the databases containing *Extension-Shearing* [1] and/or *Bending-Twisting* coupling [2] are presented as lamination parameter point clouds in Figs 2 and 3, where each point represents an individual or coincident laminate design. The use of standard ply orientations produces a feasible design space defined by a regular tetrahedron. The effect on the lamination parameter design space of applying the 10% rule is illustrated as isometric projections. The bounds of the 10% rule form a triangular plane within the feasible region when the

---

[†] Erratum:

In the published article (https://doi.org/10.1016/j.compstruct.2017.09.085), the ascending values corresponding to the '% of ±45° plies' on Fig. 1(a) are incorrect, i.e., the values appear in descending order. The values corresponding 90%, 80%, …., 10%, should therefore be replaced with 10%, 20%, …, 90%, respectively.

extensional stiffness is uncoupled, i.e. for *Bending-Twisting* coupled only designs, illustrated in Fig. 2(a) and (b), for symmetric and non-symmetric laminate designs, respectively. By contrast, bounds of the 10% rule form a reduced tetrahedron for *Extension-Shearing Bending-Twisting* coupled designs, illustrated in Fig. 2(c) and (d), for symmetric and non-symmetric laminate designs, respectively.

The corresponding lamination parameter point clouds for bending stiffness are illustrated in Fig. 3. Here, the effect of the 10% rule appears to have had limited impact on the extent of the point clouds in comparison to the fully populated designs spaces [1,2].

Additional design constraints, such as ply contiguity, are often applied in design practice. Tables 1 and 2 demonstrate the number of laminate designs for *Bending-Twisting* and *Extension-Shearing Bending-Twisting* coupled laminate designs, respectively, for different ply contiguity constraints (1, ≤2 and ≤3) within the 10% rule design space. These results reveal that the common contiguity constraint of having no more than 3 adjacent plies with the same orientation, virtually match the constraint of the 10% rule, across ply number groupings with up to (n =) 18 plies, for both symmetric and non-symmetric designs.

Orthographic projections of lamination parameter data for *Extension-Shearing Bending-Twisting* coupled designs, given in Fig. 4 for symmetric laminates and in Fig. 5 for non-symmetric laminates, provide high fidelity detail of the combined effects of the 10% rule and the ply contiguity constraint (≤3) most commonly used in aerospace applications. Each point within the 3-dimensional design space represents a physical design, for which the stacking sequences are known. These can be readily compared to the full design space, presented elsewhere [1]. It can be clearly seen that the major

impact on the reduced design space for extensional stiffness is not carried through to the design space for bending stiffness. The fact that the point cloud of individual laminate designs extends to the bounds of the feasible region will be seen to have important implications on buckling strength.

Note that the bias in the position of the lamination parameter point cloud towards the positive $\xi_{\Delta c}^{D}$ region of the design space is a result of the first (surface) ply being set to +45°; the point cloud is mirrored about the $\xi_{\Delta c}^{D}$ axis if the signs of the angle plies are switched.

2.2 Interpretation of Lamination parameter design spaces

The data illustrated in Figs 4 and 5 can be interpreted in a number of ways for the purposes of preliminary design. Lamination parameter design spaces, corresponding to the extensional stiffness data, can be interpreted through the ply percentage mapping in Fig. 1, which is an important consideration for material strength design. Lamination parameters for bending stiffness may be interpreted through a similar mapping procedure for buckling strength. The latter will help designers to understand the consequences of ignoring the effects of *Bending-Twisting* coupling in compression loaded plates as well as the potential for optimised design solutions in shear loaded plates, when common design heuristics are incorporated.

3. Buckling of Infinitely Long Plates

Bounds on the buckling performance of (infinitely) long, simply supported, 'symmetric' *Bending-Twisting* coupled laminates have been extensively investigated under both compression [6] and/or shear [4]. Hence, in view of the significant number of non-symmetric and other forms of sub-sequence symmetry recently identified [1,2], which result in a vast increase in the possible design space for *Bending-Twisting* coupled laminate designs, the possibility of additional gains in buckling performance, above symmetric laminates, can now be explored.

3.1 Closed form solution for Compression Buckling

Infinitely long compression loaded plates with simply supported edges provide a convenient lower-bound solution, and are useful for preliminary design. A closed form solution, necessary to handle the vast number of designs, can also be used to assess the buckling strength exactly:

$$N_{x,\infty} = \pi^2 \left[D_{xx} \left[\frac{1}{\lambda} \right]^2 + 2\left(D_{xy} + 2D_{ss} \right) \frac{1}{b^2} + D_{yy} \left[\frac{1}{b^4} \right] \lambda^2 \right] \tag{7}$$

For *Bending-Twisting* coupled laminates, approximate closed form solutions must be adopted [5,7], or developed.

For orthotropic laminates, the following buckling equation, representing a 2 dimensional, 4^{th} order polynomial can be solved against the exact closed form buckling solution from equally spaced points across the lamination parameter design space:

$$k_\infty = c_1 + c_2\xi_\Delta^D + c_3\xi_R^D + c_4\left(\xi_\Delta^D\right)^2 + c_5\left(\xi_R^D\right)^2 + c_6\xi_\Delta^D\xi_R^D + c_7\left(\xi_\Delta^D\right)^3 + c_8\left(\xi_R^D\right)^3 + c_9\xi_\Delta^D\left(\xi_R^D\right)^2 + c_{10}\left(\xi_\Delta^D\right)^2\xi_R^D + c_{11}\left(\xi_\Delta^D\right)^4 + c_{12}\left(\xi_R^D\right)^4 + c_{13}\xi_\Delta^D\left(\xi_R^D\right)^3 + c_{14}\left(\xi_\Delta^D\right)^2\left(\xi_R^D\right)^2 + c_{15}\left(\xi_\Delta^D\right)^3\xi_R^D \quad (8)$$

where in this case, $k_\infty = k_{x,\infty}$ and is defined by:

$$k_{x,\infty} = \frac{N_{x,\infty}b^2}{\pi^2 D_{Iso}} \quad (9)$$

Normalisation of the buckling factor, k_∞, involves the bending stiffness, D_{iso}, of the equivalent isotropic laminate, for which all lamination parameters are zero, hence:

$$D_{iso} = U_E H^3/12 \quad (10)$$

This normalisation ensures that buckling factor results are comparable across the design space; the relative change in buckling factor $k_{x\infty}$ is the same as the relative buckling load $N_{x,\infty}$. Exact buckling factor results are established at 15 sample points, corresponding to the grid point intersections formed by the equilateral triangles illustrated on the cross-section in Fig. 6(a). These results give rise to the coefficients $c_1 - c_{15}$ in Eq. (8), leading to the following closed form solution, which is applicable to all fully uncoupled laminates [12], for IM7/8552 carbon-fiber/epoxy material with Young's moduli E_1 = 161.0GPa and E_2 = 11.38GPa, shear modulus G_{12} = 5.17GPa and Poisson ratio ν_{12} = 0.38:

$$k_{x,\infty} = 4.000 - 1.049\xi_R^D - 1.217\left(\xi_\Delta^D\right)^2 + 0.340\xi_R^D\left(\xi_\Delta^D\right)^2 - 0.360\left(\xi_\Delta^D\right)^4 - 0.034\left(\xi_R^D\right)^2\left(\xi_\Delta^D\right)^2 \quad (11)$$

Equation (11) is used to develop the isolines of constant buckling factor, $k_{x,\infty}$, illustrated on Fig. 6(b). The top corners of the triangular region of Fig. 6(b), representing laminates with 90° or 0° degree plies only, have buckling factor $k_{x,\infty}$ = 1.68 (with

buckling half-waves $b/\lambda = 1.94 = (D_{yy}/D_{xx})^{1/4}$ and $\lambda/b = 1.94$, respectively), whereas the bottom corner, representing laminates with ±45° plies only, has buckling factor $k_{x,\infty} = 5.05$ (with buckling half-wave $\lambda = b$). The centre of the contour map, at which all lamination parameters are zero, represents the fully isotropic laminate and gives the classical buckling factor result, $k_{x,\infty} = 4.00$.

The 3-dimensional representation of the feasible design space in Fig. 6(a) indicates the positions through which other cross-sections are taken in order to maintain constant magnitude of *Bending-Twisting* coupling ($\xi_{\Delta c}^{D} \neq 0$). In these cases an exact infinite strip analysis [13] has been adopted to generate buckling factors at the same relative grid point locations, as illustrated on Fig. 6(a), for each discrete cross-section throughout the lamination parameter design space. This analysis was also used as a validation process for the compression buckling results. Coefficients for other cross-sections throughout the lamination parameter design space, $0 \leq \xi_{\Delta c}^{D} \leq 0.9$, are given in Table 3.

Note:

- When $\xi_{\Delta c}^{D} = \pm 1.0$, the design space degenerates to a single point with $k_{x,\infty} = 2.19$.
- Lamination parameter bounds are $-1.0 \leq \xi_{\Delta c}^{D} \leq 1.0$. Negative $\xi_{\Delta c}^{D}$ are identical to positive $\xi_{\Delta c}^{D}$.

The buckling strength relationship at any cross-section is determined by substituting the appropriate coefficients of Table 3 into Eq. (8). Note that the number of significant figures in the coefficients of Table 3 have been reduced, but are sufficient to maintain a buckling factor accurate to 2 decimal places.

3.2 Closed form solution for Shear Buckling

There are no closed form solutions for orthotropic laminates in shear, hence the following section develops new closed form solutions for shear bucking, using the exact infinite strip analysis [13] to generate buckling factors at the grid point locations illustrated on Fig. 6(a) and develop the polynomial coefficients for each slice through the lamination parameter design space, representing *Bending-Twisting* coupled designs, following the same procedure used for compression buckling in the foregoing sub-section.

For the orthotropic laminate, the closed form solution for positive and negative shear loading is identical, and is obtained by substituting the calculated coefficients from the 1st column of Tables 4 and 5, respectively, into Eq. (8).

$$\begin{aligned} k_{s,\infty} = {} & 5.336 - 2.914\xi_{\Delta}^{D} - 0.518\xi_{R}^{D} - 1.303\left(\xi_{\Delta}^{D}\right)^{2} - 0.213\left(\xi_{R}^{D}\right)^{2} + 1.048\xi_{\Delta}^{D}\xi_{R}^{D} \\ & - 0.236\left(\xi_{\Delta}^{D}\right)^{3} + 0.031\left(\xi_{R}^{D}\right)^{3} - 0.197\xi_{\Delta}^{D}\left(\xi_{R}^{D}\right)^{2} + 0.405\left(\xi_{\Delta}^{D}\right)^{2}\xi_{R}^{D} - 0.443\left(\xi_{\Delta}^{D}\right)^{4} \\ & - 0.001\left(\xi_{R}^{D}\right)^{4} + 0.022\xi_{\Delta}^{D}\left(\xi_{R}^{D}\right)^{3} - 0.185\left(\xi_{\Delta}^{D}\right)^{2}\left(\xi_{R}^{D}\right)^{2} + 0.472\left(\xi_{\Delta}^{D}\right)^{3}\xi_{\nu}^{D} \end{aligned} \tag{12}$$

where in this case, $k_{\infty} = k_{s,\infty}$ and is defined by:

$$k_{s,\infty} = \frac{N_{s,\infty} b^2}{\pi^2 D_{Iso}} \tag{13}$$

and gives the classical shear buckling factor result, $k_{s,\infty}$ = 5.34 [14], for the isotropic design, i.e., when all lamination parameters are set to zero. The resulting contour map is illustrated in Fig. 6(c), illustrating isolines of constant buckling load factor across the lamination parameter design space. Positive shear direction is defined together with

positive fibre angle direction in Fig. 6(a), for a plate of width b and infinite length (a = ∞). The top corners of the triangular region of Fig. 6(c), representing laminates with 90° and 0° degree plies only, have shear buckling factors $k_{s,\infty}$ = 4.91 and 1.31, respectively, whereas the bottom corner, representing laminates with ±45° plies only, has buckling factor $k_{s,\infty}$ = 5.61.

For *Bending-Twisting* coupled laminates, $\xi_{\Delta c}^{D} \neq 0$, coefficients for other cross-sections within the lamination parameter designs space, $0 \leq \xi_{\Delta c}^{D} \leq 0.9$, are presented in Table 4 for positive shear and Table 5 for negative shear.

Note:

- When $\xi_{\Delta c}^{D}$ = 1.0, the design space degenerates to a point with minimum and maximum $k_{s,\infty}$ = 1.38 and 8.84, for positive and negative shear, respectively.
- Lamination parameter bounds are $-1.0 \leq \xi_{\Delta c}^{D} \leq 1.0$. Negative $\xi_{\Delta c}^{D}$ produce the same effect as a reversal in the shear load direction, hence only positive $\xi_{\Delta c}^{D}$ are given.

3.3 Contour mapping

The closed form solution of Eq. (8), together with the associated coefficients of Tables 3-5, are used to develop the selection of contours maps that follow.

This contour mapping is applied to selected cross-sections through the design space, to allow detailed interrogation of the effects of *Bending-Twisting* coupling on buckling

strength. Each cross section through the tetrahedron becomes progressively smaller as the design space degenerates to a single point.

Figure 7 represents a series of compression buckling factor contour maps, corresponding to discrete and gradually increasing magnitude of *Bending-Twisting* coupling ξ_R^D = 0.1, 0.3, 0.5 and 0.7. The symmetric contours of the fully uncoupled designs, illustrated in Fig. 6(b), now give way to *increasing* asymmetry in the contour pattern. Previous work on compression loaded infinitely long plates [2] revealed that for hypothetical cases, buckling strength reduction can be up to 57%; corresponding to angle-ply only designs. The data illustrated in Fig. 5 suggests that the 10% rule does nothing to reduce this risk if the design is poorly chosen.

Figure 8 and 9 represent the equivalent series of positive and negative shear buckling factor contour maps, respectively. These reveal minima and maxima on the sloping boundary of the feasible design space. Previous work on shear buckling of infinitely long plates [1] revealed hypothetical buckling strength increase (reduction) can be up to 58% (75%), which did not take account of these local maxima (minima).

To investigate the global optima, the mapping procedure is applied to external surfaces of the feasible domain of lamination parameters, and illustrated as orthographic projections in Figs 10 and 11. These surfaces contain the upper bounds on buckling factor. The contours also reveal local optima in locations that are non-intuitive. For example: the off-centre spot height on the front and back sloping surfaces of the compression buckling contours of Figs 10(a) and (c) and; the global optimum for shear buckling corresponds to $k_{s,\infty}$ = 9.06 @ ($\xi_\Delta^D, \xi_R^D, \xi_{\Delta c}^D$) = (-0.18, -0.64, -0.82), which exceeds $k_{s,\infty}$ = 8.84 @ ($\xi_\Delta^D, \xi_R^D, \xi_{\Delta c}^D$) = (0, 1, -1) on the front (sloping) face of Fig 11(c),

corresponding to a hypothetical angle-ply only design, $[+45]_{nT}$. A practical and near optimum design from the database, $[+45_3/90/+45/90/+45/-45/0]_S$, satisfies both ply percentage and ply contiguity constraints, and leads to $k_{s,\infty}$ = 8.98 @ ($\xi_{\Delta}^{D}, \xi_{R}^{D}, \xi_{\Delta c}^{D}$) = (-0.17, -0.65, -0.80).

4. Conclusions

- The impact of the 10% rule on reducing the lamination parameter design space for extensional stiffness has been shown to be similar for both symmetric and non-symmetric designs, with standard ply orientations and up to 18 plies.
- The reduced design space, resulting from the application of the 10% rule, has been shown to virtually match to the application of the common design constraint of limiting the number of contiguous plies, i.e. adjacent plies with the same orientation, to a maximum of 3.
- No significant impact has been observed on the size of the lamination parameter design space for bending stiffness as a result of the combined effect of the 10% rule and limiting the number of contiguous plies to a maximum of 3. This implies that the upper and lower bounds on buckling strength, for both symmetric and non-symmetric designs, are not significantly affected by commonly applied heuristic design rules.
- New insights have been given for optimum compression and shear buckling strength for infinitely long plates, through the superposition of contour maps

onto the lamination parameter design space for composite laminates with *Bending-Twisting* coupling.

Acknowledgements

The Newton Research Collaboration Programme (NRCP1516/4/50) and CNPq (574004/2008-4) are gratefully acknowledged for supporting this research.

References

1 C. B. York and S. F. M. Almeida, On extension-shearing bending-twisting coupled laminates, *Composite Structures*, **164**, 2017, pp. 10-22 (doi: 10.1016/j.compstruct.2016.12.041).

2 C. B. York, On bending-twisting coupled laminates, *Composite Structures*, **160**, 2017, pp. 887-900 (doi: 10.1016/j.compstruct.2016.10.063).

3 J. A. Bailie, R. P. Ley, and A. Pasricha, *A summary and review of composite laminate design guidelines*, Task 22, NASA Contract NAS1-19347, 1997.

4 M. P. Nemeth, Buckling of symmetrically laminated plates with compression, shear, and in-plane bending, *AIAA Journal*, 30(12), 1992, pp. 2959-2965.

5 J. E. Herencia, P. M. Weaver and M. I. Friswell, Closed-form solutions for buckling of long anisotropic plates with various boundary conditions under axial compression. *Journal of Engineering Mechanics*, 136, 2010, pp. 1105-1114.

6 M. P. Nemeth, Importance of Anisotropy on Buckling of Compression-Loaded Symmetric Composite Plates, *AIAA Journal*, 24(11), 1986, pp. 1831-1835.

7 A. Baucke, C. Mittelstedt, Closed-form analysis of the buckling loads of composite laminates under uniaxial compressive load explicitly accounting for bending–twisting-coupling. *Composite Structures*, 128, 2015, pp. 437-454.

8 J. L., Grenestedt, Lay-up Optimisation against Buckling of Shear Panels, *Structural Optimisation*, 3(7), 1991, pp. 115-120.

9 H. Fukunaga, and H. Sekine, A laminate design for elastic properties of symmetric laminates with extension-shear or bending-twisting coupling, *Journal of Composite Materials*, 28(8), 1994, pp. 708-731.

10 H. Fukunaga, H. Sekine, M. Sato and A. Lino, Buckling design of symmetrically laminated plates using lamination parameters, *Computers and Structures*, 57(4), 1995, pp. 643-649.

11 S.W. Tsai and H.T. Hahn, *Introduction to composite materials*, Technomic Publishing Co. Inc., Lancaster, 1980.

12 C. B. York, Characterization of non-symmetric forms of fully orthotropic laminates, *Journal of Aircraft*, **46**(4), 2009, pp. 1114-1125 (doi:10.2514/1.32938).

13 F. W. Williams, D. Kennedy, R. Butler and M. S. Anderson, VICONOPT: Program for exact vibration and buckling analysis or design of prismatic plate assemblies. *AIAA J.* 29, 1991, pp. 1927-1928.

14 R. V. Southwell and S. W. Skan, On the stability under shear forces of a flat elastic strip, *Proceedings of the Royal Society of London*, A105, 1924, pp. 582-607.

Figures

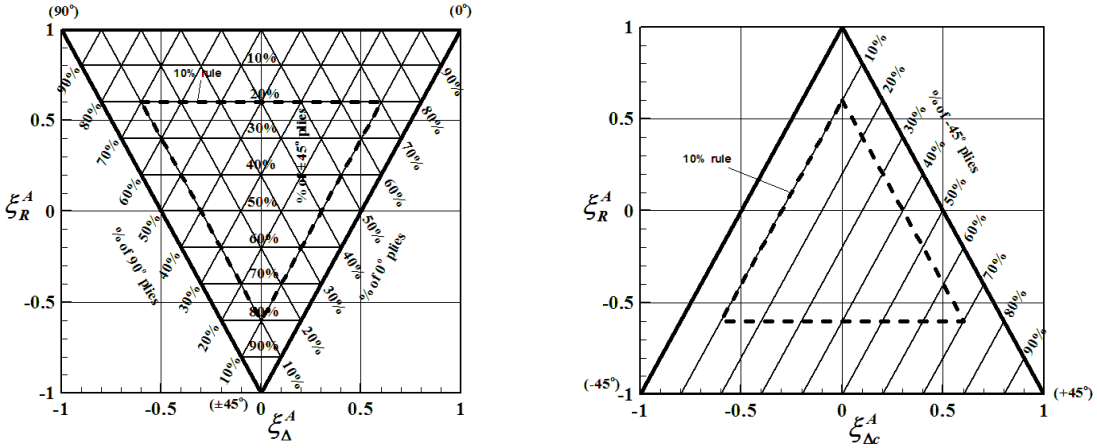

(a) (b)

Figure 1 - Lamination parameter design space with ply percentage mapping for: (a) orthotropic stiffness (ξ_{Δ}^{A} , ξ_{R}^{A}) and; (b) anisotropic stiffness ($\xi_{\Delta c}^{A}$) relating to differing angle-ply percentages. The 10% design rule constraint is also illustrated.

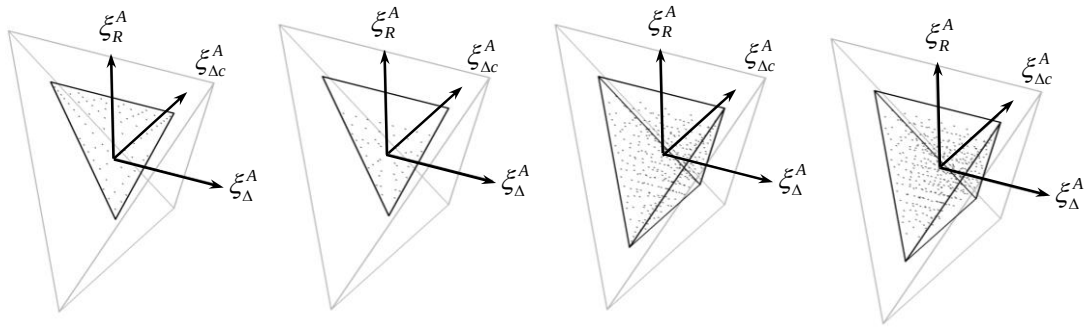

(a) (b) (c) (d)

Figure 2 - Isometric view of lamination parameter design spaces for extensional stiffness, with 10% rule applied, corresponding to: (a) Symmetric and (b) Non-symmetric *Bending-Twisting* coupled laminates with up to 18 plies and; (c) Symmetric and (d) Non-symmetric *Extension-Shearing Bending-Twisting* coupled laminates with up to 18 plies.

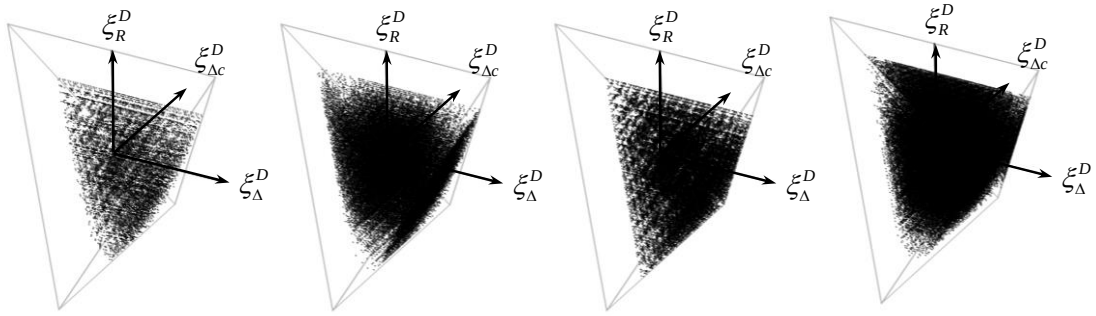

(a) (b) (c) (d)

Figure 3 - Isometric view of lamination parameter design spaces for bending stiffness, with 10% rule applied, corresponding to: (a) Symmetric and (b) Non-symmetric *Bending-Twisting* coupled laminates with up to 18 plies and; (c) Symmetric and (d) Non-symmetric *Extension-Shearing Bending-Twisting* coupled laminates with up to 18 plies.

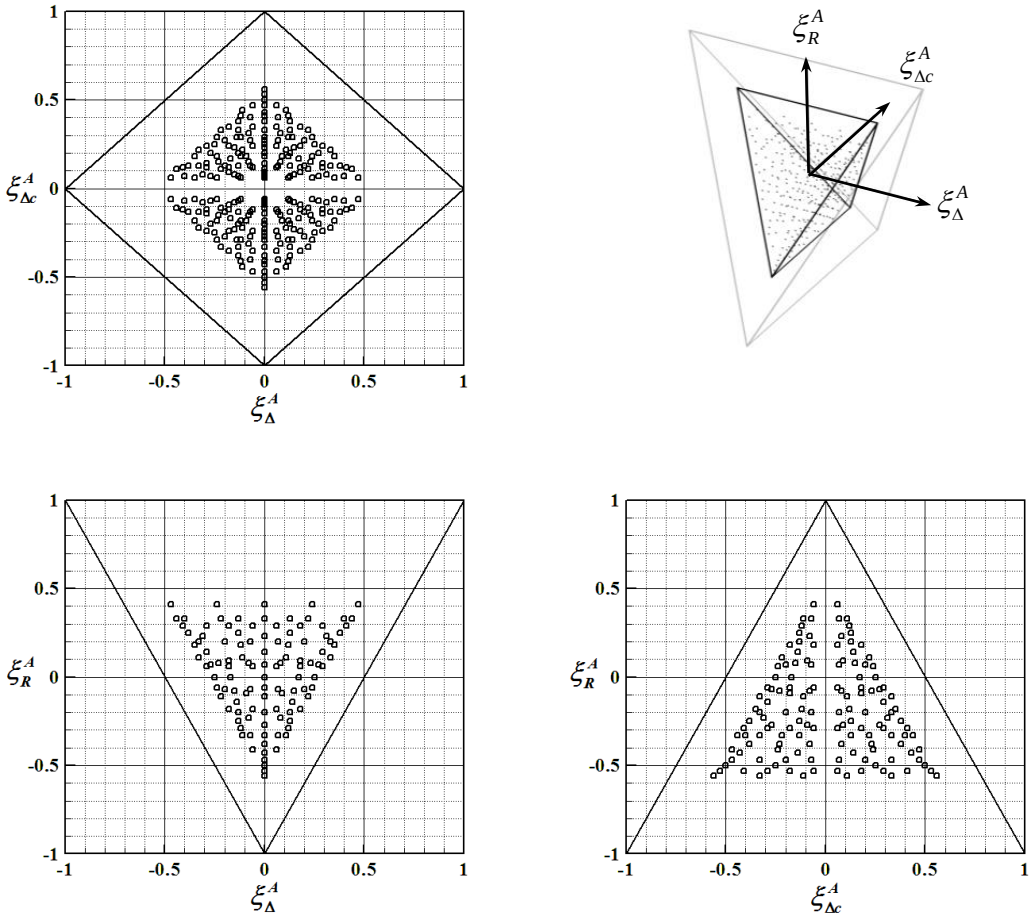

(a)

Figure 4 - Lamination parameter design spaces for symmetric *Extension-Shearing Bending-Twisting* coupled laminates with $7 \leq n \leq 18$, with 10% rule and ply contiguity constraints (≤3) applied, corresponding to isometric and orthographic projections (plan, front elevation and side elevation) for: (a) extensional stiffness ($\xi_{\Delta}^{A}, \xi_{R}^{A}, \xi_{\Delta c}^{A}$) and; (b) bending stiffness ($\xi_{\Delta}^{D}, \xi_{R}^{D}, \xi_{\Delta c}^{D}$).

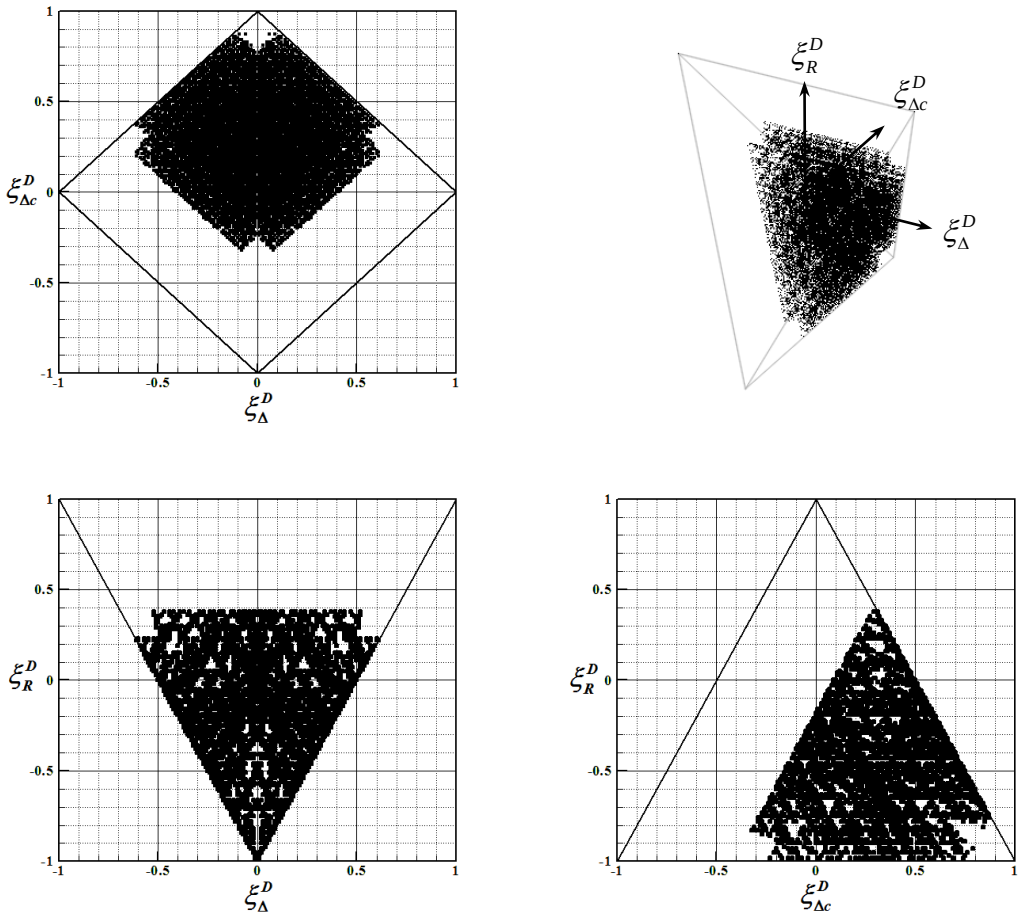
$\xi^D_{\Delta c}$
ξ^D_{Δ}
ξ^D_R
$\xi^D_{\Delta c}$
ξ^D_{Δ}
ξ^D_R
ξ^D_{Δ}
ξ^D_R
$\xi^D_{\Delta c}$

(b)

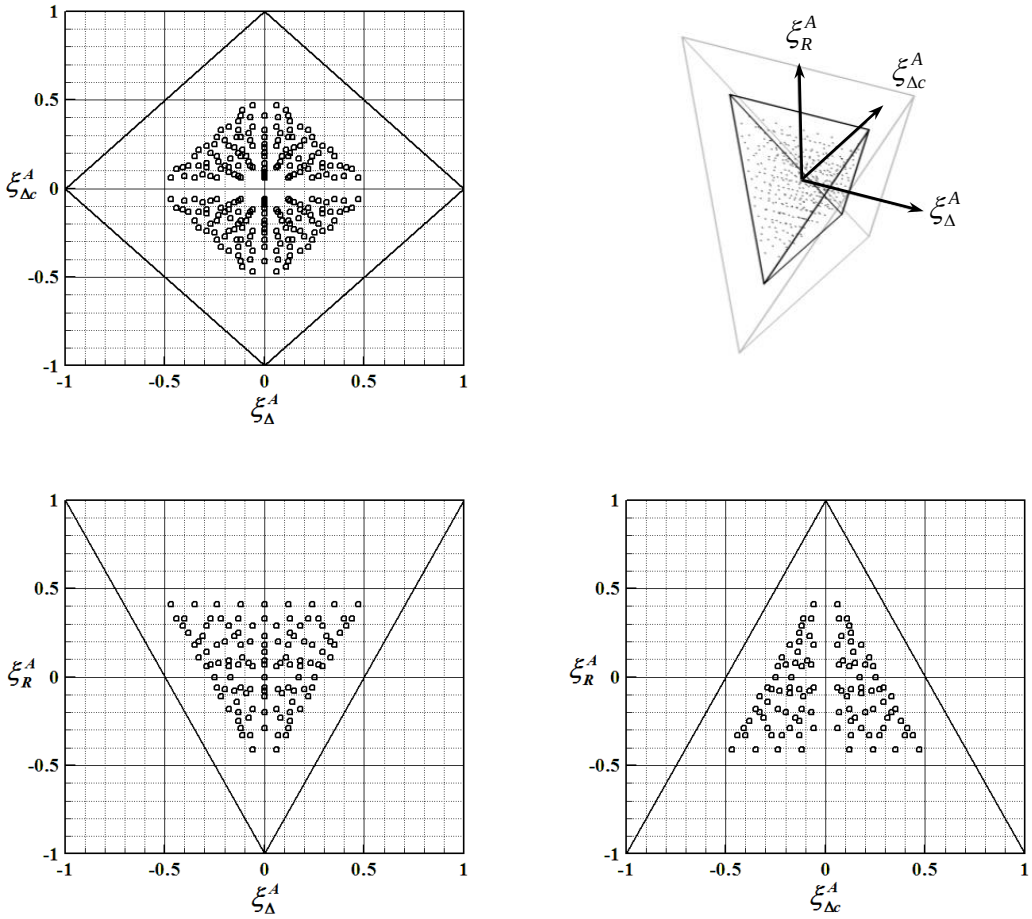

(a)

Figure 5 - Lamination parameter design spaces for non-symmetric *Extension-Shearing Bending-Twisting* coupled laminates with $7 \leq n \leq 18$, with 10% rule and ply contiguity constraints (≤3) applied, corresponding to isometric and orthographic projections (plan, front elevation and side elevation) for: (a) extensional stiffness (ξ_{Δ}^{A} , ξ_{R}^{A} , $\xi_{\Delta c}^{A}$) and; (b) bending stiffness (ξ_{Δ}^{D} , ξ_{R}^{D} , $\xi_{\Delta c}^{D}$).

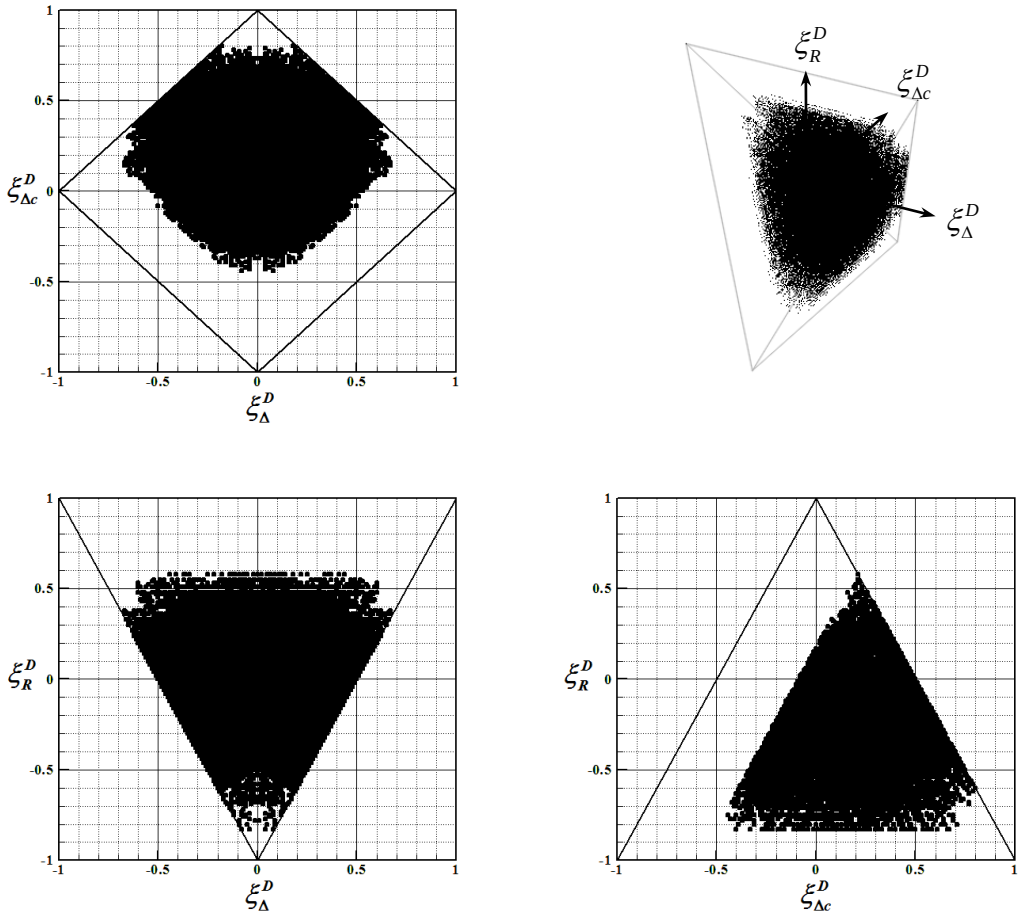
$\xi_{\Delta c}^{D}$
ξ_{Δ}^{D}
ξ_{R}^{D}
$\xi_{\Delta c}^{D}$
ξ_{Δ}^{D}
ξ_{R}^{D}
ξ_{Δ}^{D}
ξ_{R}^{D}
$\xi_{\Delta c}^{D}$

(b)

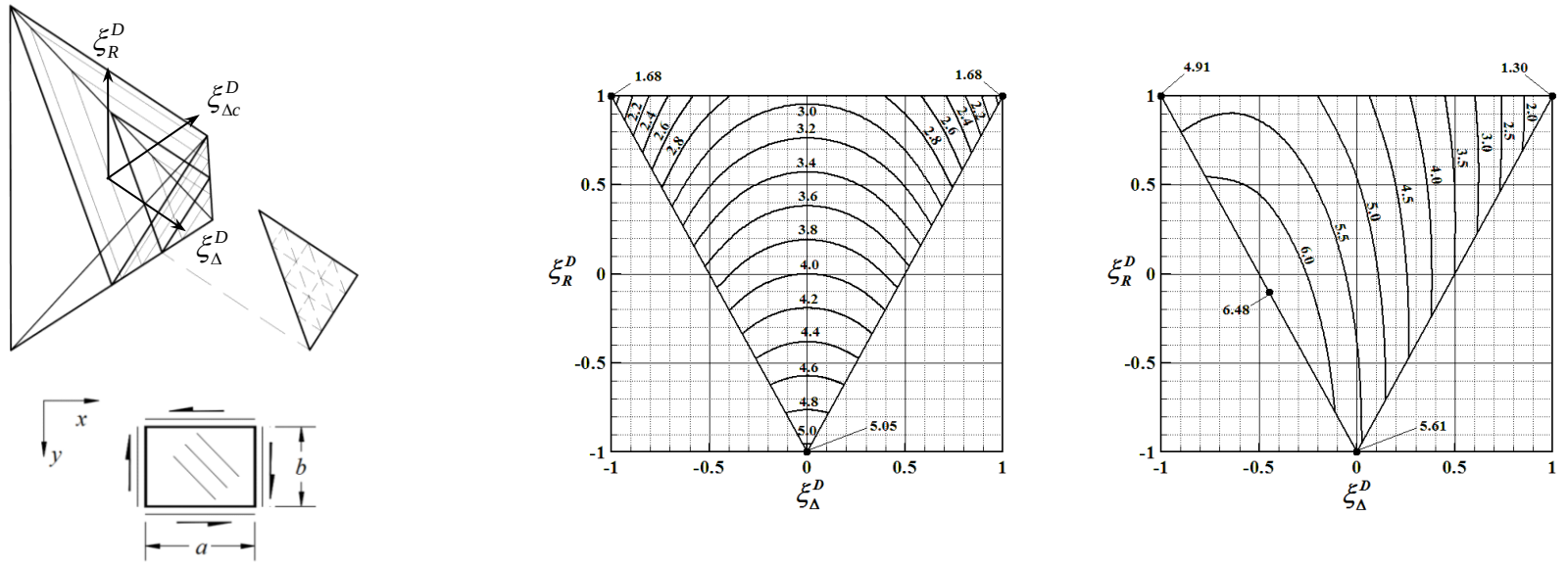

(a) (b) (c)

Figure 6 - Three-dimensional representation of the feasible design space indicating (a) the positions through which two dimensional cross-sections have been taken. Positive shear load and positive fibre orientation are defined in the thumbnail sketch. Sections representing fully uncoupled laminates [12] in bending, correspond to: (b) compression buckling contours, $k_{x,\infty}$ (= $N_x b^2/\pi^2 D_{Iso}$) and; (c) positive/negative shear buckling contours, $k_{s,\infty}$ (= $N_s b^2/\pi^2 D_{Iso}$).

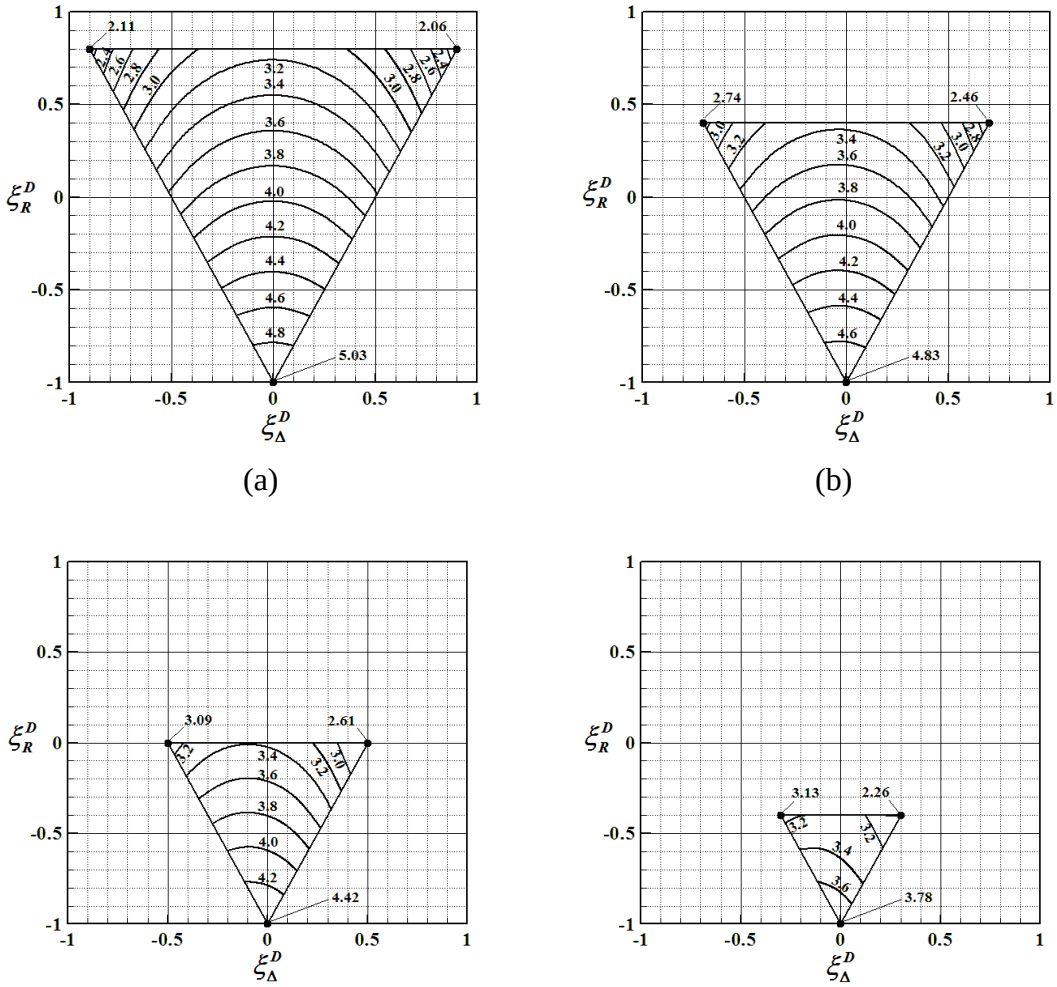

Figure 7 - Compression buckling factor contours, $k_{x,\infty}$ (= $N_x b^2/\pi^2 D_{Iso}$), for: (a) $\xi^D_{\Delta c}$ = 0.1: $\xi^D_{\Delta c}$ = 0.3, $\xi^D_{\Delta c}$ = 0.5 and $\xi^D_{\Delta c}$ = 0.7, representing *Bending-Twisting* coupled laminates.

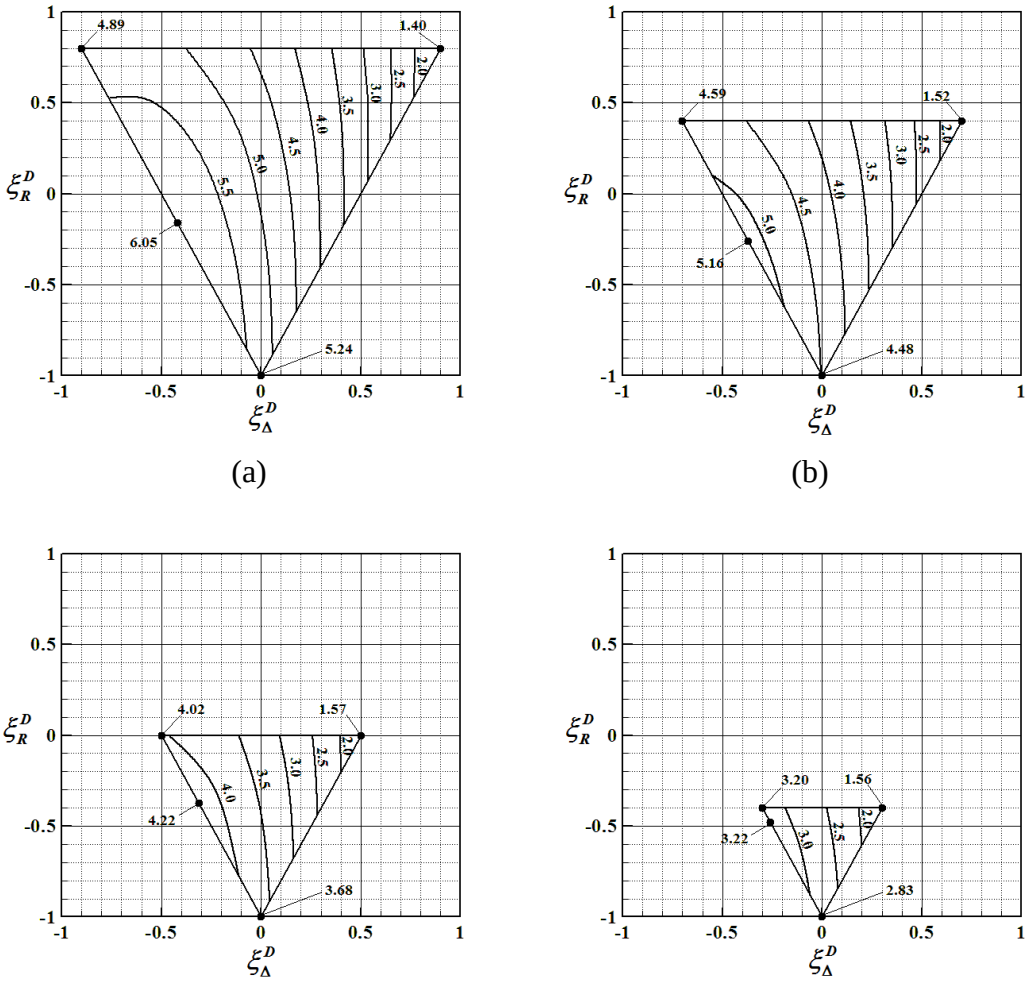

Figure 8 - Positive shear buckling factor contours, $k_{s,\infty}$ (= $N_s b^2/\pi^2 D_{Iso}$), for: (a) $\xi_{\Delta c}^D$ = 0.1: $\xi_{\Delta c}^D$ = 0.3, $\xi_{\Delta c}^D$ = 0.5 and $\xi_{\Delta c}^D$ = 0.7, representing *Bending-Twisting* coupled laminates.

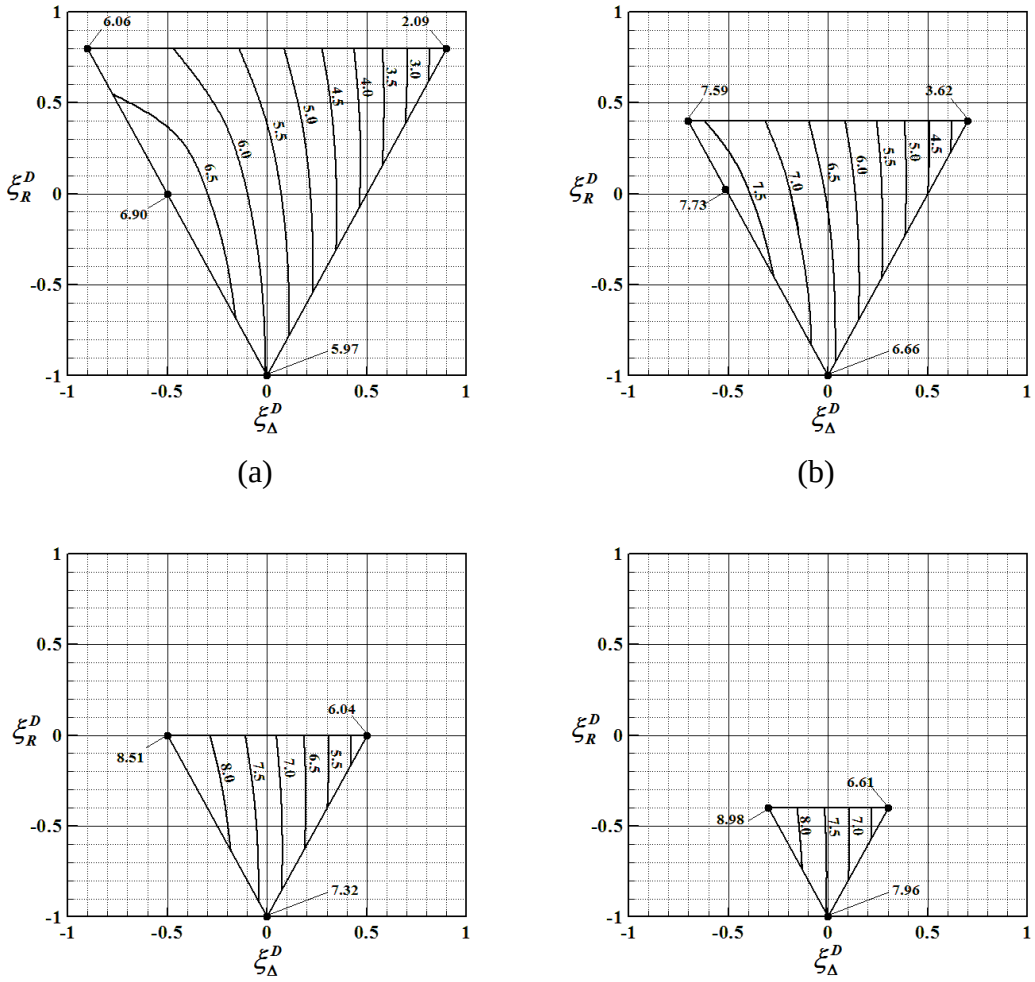

Figure 9 - Negative shear buckling factor contours, $k_{s,\infty}$ (= $N_s b^2/\pi^2 D_{Iso}$), for: (a) $\xi_{\Delta c}^D$ = 0.1: $\xi_{\Delta c}^D$ = 0.3, $\xi_{\Delta c}^D$ = 0.5 and $\xi_{\Delta c}^D$ = 0.7, representing *Bending-Twisting* coupled laminates.

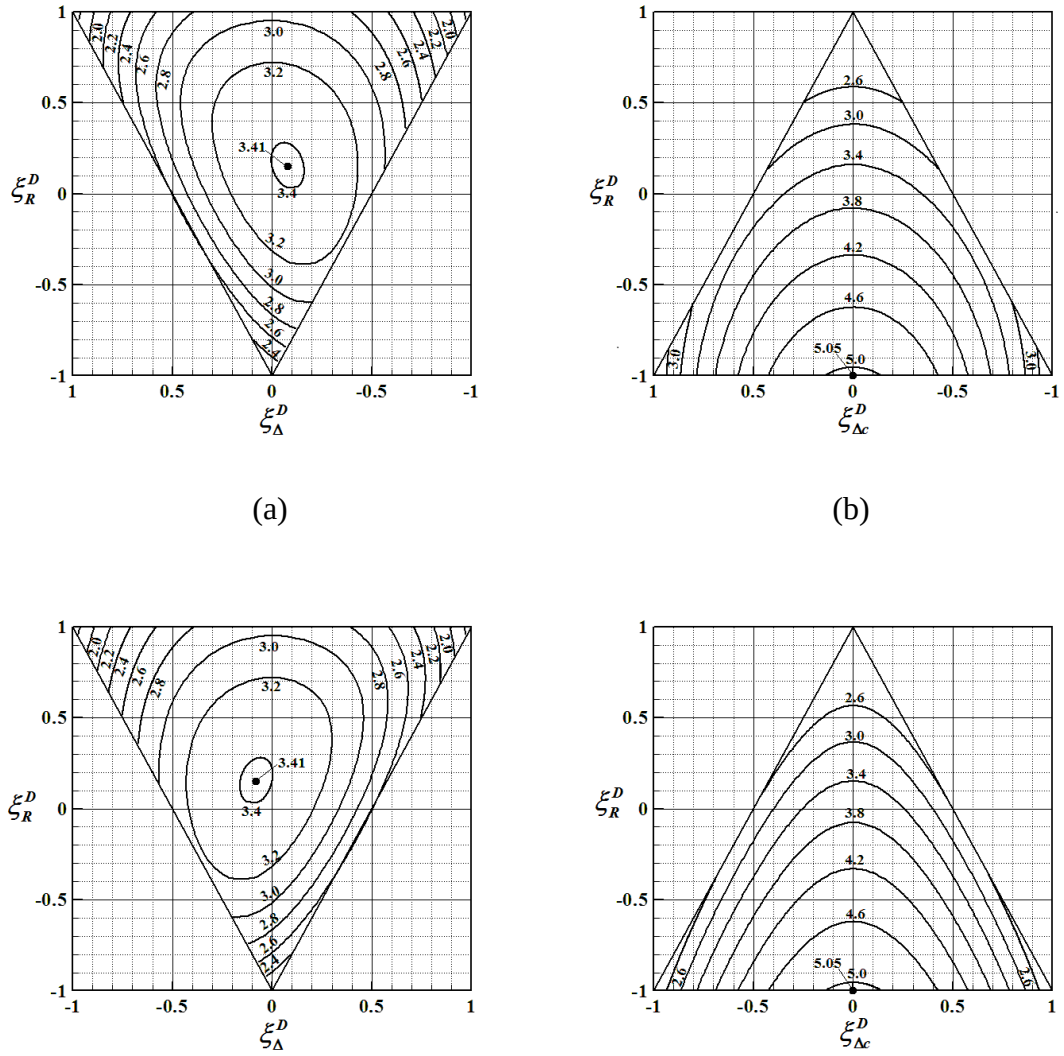

Figure 10 - Lamination parameter design space surface contours for Compression buckling factor, $k_{x,\infty}$ (= $N_x b^2/\pi^2 D_{Iso}$), corresponding to 3rd angle orthographic projections of: (a) Rear (sloping) face with; (b) Left (sloping) face; (c) Front (sloping) face and; Right (sloping) face.

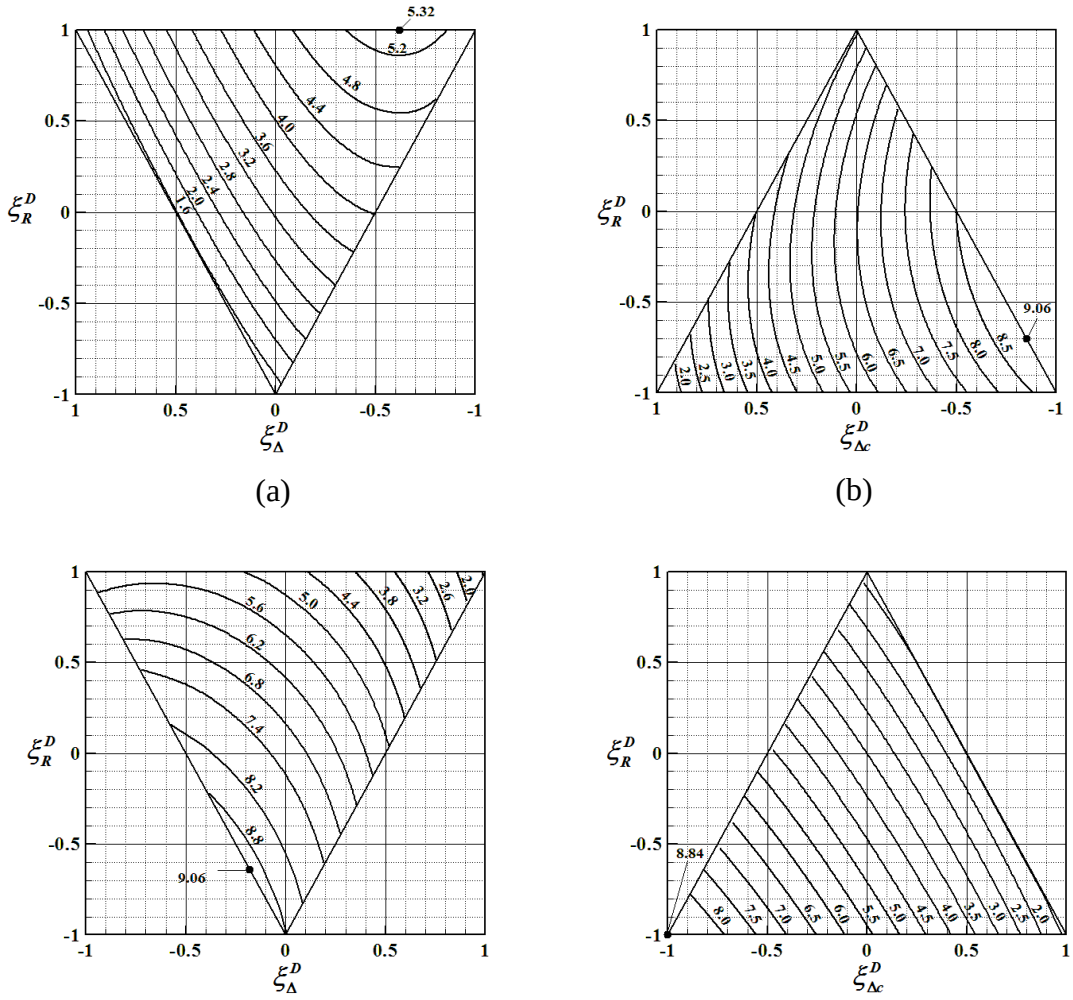

Figure 11 - Lamination parameter design space surface contours for Positive Shear buckling factor, $k_{s,\infty}$ (= $N_s b^2/\pi^2 D_{Iso}$), corresponding to 3rd angle orthographic projections of: (a) Rear (sloping) face; (b) Left (sloping) face; (c) Front (sloping) face and; Right (sloping) face.

Table 1 – Effect of ply contiguity constraints on the 10% rule design space for: (a) Symmetric and; (b) Non-symmetric *Bending-Twisting* coupled laminates.

	(a) Symmetric laminates				(b) Non-symmetric laminates			
n	1	≤2	≤3	10%	1	≤2	≤3	10%
7	4	-	-	4	-	-	-	-
8	-	6	-	6	-	-	-	-
9	10	14	18	18	-	-	-	-
10	-	20	-	24	-	-	-	-
11	14	30	44	48	8	14	16	16
12	-	96	104	128	-	-	-	-
13	68	164	242	260	38	216	272	276
14	-	422	-	534	36	204	220	224
15	240	676	980	1,080	232	2,746	3,628	3,734
16	-	1,572	1,790	2,302	158	2,064	2,734	2,868
17	690	2,736	4,184	4,612	1,480	27,716	39,258	41,142
18	-	6,000	7,142	9,324	826	21,180	31,568	34,154

Table 2 – Effect of ply contiguity constraints on the 10% rule design space for: (a) Symmetric and; (b) Non-symmetric *Extension-Shearing Bending-Twisting* coupled laminates.

	(a) Symmetric laminates				(b) Non-symmetric laminates			
n	1	≤2	≤3	10%	1	≤2	≤3	10%
7	2	-	-	2	-	-	-	-
8	-	-	-	-	-	-	-	-
9	26	40	42	42	4	8	-	8
10	-	34	-	36	-	-	-	-
11	94	150	190	192	8	38	48	48
12	-	214	224	260	8	32	36	36
13	382	934	1,258	1,300	146	916	1,240	1,292
14	-	1,114	1,264	1,560	36	412	560	592
15	1,380	4,796	6,940	7,320	924	14,212	19,970	21,152
16	-	5,104	6,102	7,882	266	5,554	8,498	9,288
17	4,720	21,840	33,478	36,176	6,582	165,022	251,098	270,848
18	-	22,016	27,772	37,212	1,896	62,632	102,178	114,638

Table 3 – Compression buckling coefficients for Eq. (8) for $0 \leq \xi_{\Delta c}^{D} < 1.0$.

	$\xi_{\Delta c}^{D}$									
	0	.1	.2	.3	.4	.5	.6	.7	.8	.9
c_1	4.000	3.976	3.903	3.781	3.606	3.374	3.078	2.708	2.198	1.903
c_2	0.000	-0.014	-0.054	-0.119	-0.210	-0.329	-0.481	-0.674	-0.905	-1.384
c_3	-1.049	-1.049	-1.049	-1.050	-1.053	-1.060	-1.078	-1.099	-1.369	-0.042
c_4	-1.217	-1.235	-1.291	-1.391	-1.539	-1.742	-2.012	-2.395	-3.022	-2.872
c_5	0.000	0.000	-0.001	-0.003	-0.006	-0.012	-0.024	-0.008	-0.421	2.058
c_6	0.000	0.007	0.027	0.057	0.098	0.145	0.195	0.229	0.300	-0.358
c_7	0.000	-0.014	-0.073	-0.185	-0.360	-0.598	-0.894	-1.195	-1.324	-1.151
c_8	0.000	-0.001	0.000	-0.001	-0.001	-0.001	-0.004	0.029	-0.299	1.621
c_9	0.000	0.004	0.009	0.009	0.003	-0.014	-0.044	-0.108	-0.114	-1.027
c_{10}	0.340	0.351	0.390	0.452	0.542	0.671	0.843	0.997	0.975	3.589
c_{11}	-0.360	-0.399	-0.509	-0.697	-0.993	-1.456	-2.213	-3.501	-5.882	-11.944
c_{12}	0.000	0.000	0.000	0.000	0.000	0.000	-0.001	0.012	-0.092	0.451
c_{13}	0.000	-0.002	-0.003	-0.004	-0.004	-0.003	0.001	0.003	0.055	-0.238
c_{14}	-0.034	-0.032	-0.041	-0.052	-0.066	-0.083	-0.127	-0.262	-0.581	0.594
c_{15}	0.000	-0.018	-0.047	-0.068	-0.065	-0.008	0.159	0.561	1.484	3.064

Table 4 – Positive shear buckling coefficients for Eq. (8) for $0 \leq \xi_{\Delta c}^{D} < 0.9$.

	$\xi_{\Delta c}^{D}$									
	0	.1	.2	.3	.4	.5	.6	.7	.8	.9
c_1	5.336	4.943	4.539	4.123	3.693	3.245	2.776	2.279	1.701	1.356
c_2	-2.914	-2.841	-2.761	-2.675	-2.581	-2.476	-2.354	-2.203	-1.971	-1.822
c_3	-0.518	-0.542	-0.57	-0.602	-0.64	-0.685	-0.741	-0.808	-1.106	-0.02
c_4	-1.303	-1.332	-1.372	-1.423	-1.493	-1.591	-1.738	-1.985	-2.425	-1.929
c_5	-0.213	-0.211	-0.21	-0.208	-0.206	-0.205	-0.206	-0.191	-0.565	1.597
c_6	1.048	1.059	1.073	1.089	1.109	1.135	1.174	1.245	1.487	1.082
c_7	-0.236	-0.183	-0.132	-0.073	0.006	0.12	0.3	0.591	1.1	1.212
c_8	0.031	0.031	0.033	0.036	0.04	0.044	0.049	0.075	-0.22	1.476
c_9	-0.197	-0.19	-0.191	-0.197	-0.205	-0.211	-0.216	-0.204	-0.016	-0.809
c_{10}	0.405	0.363	0.332	0.301	0.257	0.187	0.064	-0.195	-0.657	1.608
c_{11}	-0.443	-0.469	-0.516	-0.586	-0.687	-0.831	-1.044	-1.367	-1.873	-3.69
c_{12}	-0.001	0.001	0.001	0.002	0.003	0.003	0.004	0.013	-0.08	0.406
c_{13}	0.022	0.016	0.013	0.01	0.01	0.014	0.015	0.023	0.103	-0.26
c_{14}	-0.185	-0.176	-0.179	-0.194	-0.223	-0.263	-0.332	-0.469	-0.65	0.901
c_{15}	0.472	0.487	0.523	0.584	0.672	0.804	1.001	1.286	1.739	1.455

Table 5 – Negative shear buckling coefficients for Eq. (8) for $0 \leq \xi_{\Delta c}^{D} < 0.9$.

	$\xi_{\Delta c}^{D}$									
	0	.1	.2	.3	.4	.5	.6	.7	.8	.9
c_1	5.336	5.719	6.092	6.456	6.811	7.157	7.495	7.825	8.119	8.624
c_2	-2.914	-2.999	-3.074	-3.146	-3.218	-3.291	-3.369	-3.452	-3.516	-3.987
c_3	-0.518	-0.488	-0.464	-0.443	-0.424	-0.406	-0.389	-0.363	-0.489	0.431
c_4	-1.303	-1.293	-1.283	-1.273	-1.264	-1.256	-1.252	-1.261	-1.284	0.574
c_5	-0.213	-0.214	-0.216	-0.218	-0.218	-0.220	-0.219	-0.199	-0.481	1.100
c_6	1.048	1.047	1.044	1.040	1.034	1.025	1.012	0.999	1.099	-0.324
c_7	-0.236	-0.227	-0.254	-0.295	-0.339	-0.385	-0.421	-0.442	-0.429	-1.614
c_8	0.031	0.024	0.022	0.020	0.020	0.020	0.021	0.040	-0.203	1.024
c_9	-0.197	-0.163	-0.153	-0.155	-0.160	-0.165	-0.178	-0.187	-0.035	-1.803
c_{10}	0.405	0.353	0.354	0.374	0.403	0.436	0.469	0.466	0.464	4.874
c_{11}	-0.443	-0.370	-0.346	-0.353	-0.386	-0.449	-0.551	-0.702	-0.902	-2.378
c_{12}	-0.001	0.000	0.001	0.000	0.000	0.000	0.000	0.007	-0.072	0.284
c_{13}	0.022	0.011	0.007	0.007	0.009	0.015	0.017	0.024	0.104	-0.616
c_{14}	-0.185	-0.134	-0.116	-0.114	-0.123	-0.135	-0.158	-0.221	-0.266	2.259
c_{15}	0.472	0.368	0.326	0.319	0.335	0.381	0.466	0.579	0.746	-0.588

Figure Captions

Figure 1 - Lamination parameter design space with ply percentage mapping for: (a) orthotropic stiffness (ξ_{Δ}^{A} , ξ_{R}^{A}) and; (b) anisotropic stiffness ($\xi_{\Delta c}^{A}$) relating to differing angle-ply percentages. The 10% design rule constraint is also illustrated.

Figure 2 - Isometric view of lamination parameter design spaces for extensional stiffness, with 10% rule applied, corresponding to: (a) Symmetric and (b) Non-symmetric *Bending-Twisting* coupled laminates with up to 18 plies and; (c) Symmetric and (d) Non-symmetric *Extension-Shearing Bending-Twisting* coupled laminates with up to 18 plies.

Figure 3 - Isometric view of lamination parameter design spaces for bending stiffness, with 10% rule applied, corresponding to: (a) Symmetric and (b) Non-symmetric *Bending-Twisting* coupled laminates with up to 18 plies and; (c) Symmetric and (d) Non-symmetric *Extension-Shearing Bending-Twisting* coupled laminates with up to 18 plies.

Figure 4 - Lamination parameter design spaces for symmetric *Extension-Shearing Bending-Twisting* coupled laminates with $7 \leq n \leq 18$, with 10% rule and ply contiguity constraints (≤3) applied, corresponding to isometric and orthographic projections (plan, front elevation and side elevation) for: (a) extensional stiffness (ξ_{Δ}^{A} , ξ_{R}^{A} , $\xi_{\Delta c}^{A}$) and; (b) bending stiffness (ξ_{Δ}^{D} , ξ_{R}^{D} , $\xi_{\Delta c}^{D}$).

Figure 5 - Lamination parameter design spaces for non-symmetric *Extension-Shearing Bending-Twisting* coupled laminates with $7 \leq n \leq 18$, with 10% rule and ply contiguity constraints (≤3) applied, corresponding to isometric and orthographic projections (plan,

front elevation and side elevation) for: (a) extensional stiffness (ξ_{Δ}^{A} , ξ_{R}^{A} , $\xi_{\Delta c}^{A}$) and; (b) bending stiffness (ξ_{Δ}^{D} , ξ_{R}^{D} , $\xi_{\Delta c}^{D}$).

Figure 6 - Three-dimensional representation of the feasible design space indicating (a) the positions through which two dimensional cross-sections have been taken. Positive shear load and positive fibre orientation are defined in the thumbnail sketch. Sections representing fully uncoupled laminates [12] in bending, correspond to: (b) compression buckling contours, $k_{x,\infty}$ (= $N_x b^2/\pi^2 D_{Iso}$) and; (c) positive/negative shear buckling contours, $k_{s,\infty}$ (= $N_s b^2/\pi^2 D_{Iso}$).

Figure 7 - Compression buckling factor contours, $k_{x,\infty}$ (= $N_x b^2/\pi^2 D_{Iso}$), for: (a) $\xi_{\Delta c}^{D}$ = 0.1: $\xi_{\Delta c}^{D}$ = 0.3, $\xi_{\Delta c}^{D}$ = 0.5 and $\xi_{\Delta c}^{D}$ = 0.7, representing *Bending-Twisting* coupled laminates.

Figure 8 - Positive shear buckling factor contours, $k_{s,\infty}$ (= $N_s b^2/\pi^2 D_{Iso}$), for: (a) $\xi_{\Delta c}^{D}$ = 0.1: $\xi_{\Delta c}^{D}$ = 0.3, $\xi_{\Delta c}^{D}$ = 0.5 and $\xi_{\Delta c}^{D}$ = 0.7, representing *Bending-Twisting* coupled laminates.

Figure 9 - Negative shear buckling factor contours, $k_{s,\infty}$ (= $N_s b^2/\pi^2 D_{Iso}$), for: (a) $\xi_{\Delta c}^{D}$ = 0.1: $\xi_{\Delta c}^{D}$ = 0.3, $\xi_{\Delta c}^{D}$ = 0.5 and $\xi_{\Delta c}^{D}$ = 0.7, representing *Bending-Twisting* coupled laminates.

Figure 10 - Lamination parameter design space surface contours for Compression buckling factor, $k_{x,\infty}$ (= $N_x b^2/\pi^2 D_{Iso}$), corresponding to 3rd angle orthographic projections of: (a) Rear (sloping) face with; (b) Left (sloping) face; (c) Front (sloping) face and; Right (sloping) face.

Figure 11 - Lamination parameter design space surface contours for Positive Shear buckling factor, $k_{s,\infty}$ (= $N_s b^2/\pi^2 D_{Iso}$), corresponding to 3rd angle orthographic projections

of: (a) Rear (sloping) face; (b) Left (sloping) face; (c) Front (sloping) face and; Right (sloping) face.